Dolomites Research Notes on Approximation

Special Issue SA2022 – *Software for Approximation 2022*, Volume 15 · 2022 · Pages 92–100

CQMC: an improved code for low-dimensional Compressed Quasi-MonteCarlo cubature*

Giacomo Elefante[a] · Alvise Sommariva[a] · Marco Vianello[a]

Abstract

An improved version of Compressed Quasi-MonteCarlo cubature (CQMC) on large low-discrepancy samples is implemented, on 2D and 3D regions with complex shape. The algorithms rests on the concept of Tchakaloff set and on NNLS solution of a sequence of "small" moment-matching systems. Examples of area and volume integration are provided.

1 Introduction

The need for cubature formulas on low-dimensional regions with complex shape has been manifestly emerging in the last years, especially in the framework of FEM and VEM with curved elements. A typical 2D instance is the intersection (or difference with holes) of a polygonal element with a curved boundary domain, possibly shaped by splines or NURBS, where accurate tracking of the resulting element boundary could be very difficult. Even more difficult instances arise with 3D curved polyhedral elements, where boundary tracking becomes often challenging; we may quote among others, without any pretence of exhaustivity, [1, 2, 3, 6, 27, 28] with the references therein.

On the other hand, complex integration shapes could arise in several different contexts, such as for example Lagrangian flux calculation through a fixed curve/surface for scalar conservation laws [36], obscured and vignetted lens configurations in optical design for astronomy [4, 5], union of several overlapping balls in molecular modelling [23], and many others.

A general purpose but partially overlooked solution to the problem of tracking complex shapes comes from QMC (Quasi-MonteCarlo) cubature formulas, whenever an implementation of the indicator function for the integration domain is available (indeed, QMC cubature was mainly thought for high-dimensional integration on standard domains such as cubes and spheres). We recall that a QMC cubature formula on a compact domain $\Omega \subset \mathbb{R}^d$ corresponds to a equal-masses discrete measure such that

$$Q(f) = \frac{vol(\Omega)}{N} \sum_{i=1}^{N} f(x_i) \approx I(f) = \int_\Omega f(x)\,dx \tag{1}$$

where the points $X = \{x_1, \ldots, x_N\} \subset \Omega$ are taken from a low-discrepancy sequence, like e.g. Halton and Sobol points. As it is well-known, roughly the error of QMC formulas with such sampling sequences is close to $\mathcal{O}(1/N)$, under mild regularity assumptions on the integrand f (whereas MC formulas have a probabilistic error $\mathcal{O}(1/\sqrt{N})$). We do not even attempt to recall the main thoretical and computational aspects of QMC integration, based on notions and results like discrepancy and star-discrepancy, Hardy-Krause variation, the Koksma-Hlawka and Erdös-Turán-Koksma inequalities, for which refer to relevant and comprehensive surveys such as [8, 9, 17, 22].

The possible drawback arising when high accuracy is required, i.e. the need of huge low-discrepancy samples, can be coped using suitable cubature compression techniques. Indeed, a first step with QMC formulas on low-dimensional complex shapes was made in [7], following the compression method for multivariate discrete measures introduced in [29] and later perfected in [25], which is based on Caratheodory-Tchakaloff subsampling. The method essentially works as follows: given a discrete measure with support $X = \{x_i\} \subset \mathbb{R}^d$ and point masses $\{\lambda_i\}$, $1 \le i \le N$, and defining

$$V(X) = V_n(X) = (p_j(x_i)) \in \mathbb{R}^{N\times r}\,,\ \ N > r\,, \tag{2}$$

$1 \le i \le N = card(X)$, $1 \le j \le r = dim(\mathbb{P}^d_n(X))$, the Vandermonde-like matrix with respect to a total-degree basis $\{p_j\}$ for the d-variate polynomials of degree not exceeding n restricted to X, one seeks a sparse nonnegative solution to the underdetermined moment-matching system

$$V^t(X)u = m_X\,,\ \ u \ge 0\,, \tag{3}$$

where $m_X = V^t(X)\lambda = \{Q(p_j)\}$, as a NonNegative Least-Squares (NNLS) problem

$$\min\{\|V^t(X)u - m_X\|_2\,, u \in \mathbb{R}^r\,, u \ge 0\}\,. \tag{4}$$

Existence of a nonnegative solution with a number of nonzeros not exceeding r is guaranteed by the famous Caratheodory theorem on finite-dimensional conic combinations, applied to the columns of $V^t(X)$. When (X, λ) is itself an algebraic cubature

*The preface of this special issue to which the article belongs is given in [12].

[a]Department of Mathematics, University of Padova, Italy

formula on Ω, this is nothing but Tchakaloff theorem on the existence of positive algebraic cubatures [33]. Observe that denoting by $w = \{w_k = u_{i_k} : u_{i_k} > 0\}$ and $T = \{t_k = x_{i_k} : u_{i_k} > 0\}$, the original discrete measure is compressed into a measure (T, w) with possibly much smaller support $T \subseteq X$, such that

$$V^t(T)w = m_X \, , \; w \in \mathbb{R}^\nu \, , \; \nu \le r \, , \tag{5}$$

or equivalently

$$\sum_{k=1}^{\nu} w_k \, p(t_k) = \sum_{i=1}^{N} \lambda_i \, p(x_i) \, , \;\; \forall p \in \mathbb{P}^d_n(X) \, , \tag{6}$$

where typically $\nu \le r \ll N$, i.e. a substantial compression of the measure has been obtained.

On the other hand, the NNLS problem can be conveniently solved via Lawson-Hanson active set iterative algorithm [20]. It is worth recalling that the problem of computing a sparse nonnegative solution to the underdetermined moment system $V^t u = m$, has attracted some attention in the last decade in both the probabilistic and deterministic framework. Indeed, it can be solved also by other strategies, for example by Linear Programming (LP) instead of Quadratic Programming: we may quote [19, 21, 26, 34] with the references therein. Nevertheless, in our numerical experience the NNLS approach has shown to be less time consuming than the LP approach (at least in the Matlab environment), so it has been adopted in all our relevant codes, for example in [25], where we refer the interested reader for some comparisons.

In the sequel we shall assume that the discrete set $X \subset \Omega$ is determining for the polynomials of degree not exceeding n, i.e.

$$r = dim(\mathbb{P}^d_n(X)) = dim(\mathbb{P}^d_n) = \binom{n+d}{d} \tag{7}$$

(or equivalently polynomials in $\mathbb{P}^d_n$ vanishing on X vanish everywhere). This is not really restrictive since, as discussed in [14], with $N \ge dim(\mathbb{P}^d_n)$ uniformly distributed points in a volume the probability that the corresponding Vandermonde matrix has not full rank is zero. From a deterministic point of view, we may also observe that if Ω satisfies a Markov polynomial inequality, for example if Ω satisfies an interior cone condition, then a low-discrepancy sequence X is even a norming set for $\mathbb{P}^d_n$ on Ω (and thus obviously $\mathbb{P}^d_n$-determining) as soon as X has a sufficiently small fill distance, i.e., if N is sufficiently large; cf. e.g. [10] for a survey of such notions and results on polynomial inequalities.

Let us now turn to the QMC cubature framework. In this case we have simply $\lambda_i = vol(\Omega)/N$ for every i, the compressed formula will be denoted by

$$Q_c(f) = \sum_{k=1}^{\nu} w_k \, f(t_k) \approx I(f) = \int_\Omega f(x)\, dx \, , \tag{8}$$

and property (6) reads

$$Q_c(p) = \sum_{k=1}^{\nu} w_k \, p(t_k) = Q(p) = \frac{vol(\Omega)}{N} \sum_{i=1}^{N} p(x_i) \, , \;\; \forall p \in \mathbb{P}^d_n \, . \tag{9}$$

In order to give an error estimate for the compressed cubature, let p^*_n denote the best approximation polynomial to a continuous function f in the uniform norm on Ω, that is

$$\|f - p^*_n\|_{\infty,\Omega} = E_n(f;\Omega) = \min_{p \in \mathbb{P}^d_n} \|f - p\|_{\infty,\Omega} \, . \tag{10}$$

Then we can write the chain of inequalities

$$\begin{aligned} |I(f) - Q_c(f)| &\le |I(f) - Q(f)| + |Q(f) - Q_c(f)| \, , \\ |Q(f) - Q_c(f)| &\le |Q(f) - Q(p^*_n)| + |Q(p^*_n) - Q_c(p^*_n)| + |Q_c(p^*_n) - Q_c(f)| \\ &\le |I(f) - Q(f)| + \left(\frac{vol(\Omega)}{N} N + \sum_{k=1}^{\nu} w_k \right) E_n(f;\Omega) \, , \end{aligned} \tag{11}$$

that is we get the error bound

$$|I(f) - Q_c(f)| \le |I(f) - Q(f)| + 2\, vol(\Omega)\, E_n(f;\Omega) \, , \tag{12}$$

where we have used the fact that $Q(p^*_n) - Q_c(p^*_n) = 0$ in view of (9), and that both Q and Q_c have positive weights whose sum equals $vol(\Omega)$ (by exactness on constant polynomials).

We recall that the rate of $E_n(f;\Omega)$ can be estimated depending on the regularity of f as soon as Ω is a so-called "Jackson compact set", i.e. a Jackson like inequality is available on Ω. This means that for every $s > 0$ there exists a positive integer α_s such that for $f \in C^{\alpha_s}(\Omega)$ there exists a constant $C_s(f)$ (depending on the partial derivatives of f up to order α_s) for which $E_n(f;\Omega) \le C_s(f)\, n^{-s}$ holds for $n > s$. Examples are hypercubes with $\alpha_s = s + 1$ and balls with $\alpha_s = s$. The class is wide, including e.g. all subanalytic sets, that are finite union of real analytic images of hypercubes; cf. [24] for a survey on the multivariate Jackson inequality.

The meaning of inequality (12) is that, up to a quantity proportional to $E_n(f;\Omega)$, the compressed QMC formula retains the approximation power of the original QMC formula, but using a much lower number of samples. On the other hand, by (9) it retains exactly the same approximation power of the original QMC formula on polynomials in $\mathbb{P}^d_n$, having the same polynomial moments up to degreee n. As we shall see in the numerical tests, in 2D and 3D this entails that a compressed sample of tens or hundreds of points could substitute a huge sample of a million points for sufficiently regular functions.

2 Improving compressed QMC cubature

A further step in the improvement of low-dimensional QMC compression on complex shapes, can by obtained via the notion of "Tchakaloff set", formally introduced by Wilhelmsen in 1976 following previous work by Davis on the proof of Tchakaloff theorem, cf. [13, 35]. Indeed, consider a finite-dimensional function space $S = span\{p_1, \ldots, p_r\}$, $r = dim(S)$, on a compact domain $\Omega \subset R^d$, satisfying the "Krein condition", i.e. there exists a function in S not vanishing on Ω (e.g., a polynomial space). Let L be a strictly positive linear functional on S, i.e. $L(p) > 0$ for every $p \in S$, $p \geq 0$ not identically vanishing on Ω. A Tchakaloff set for L on S is a subset, say $\mathcal{T} \subset \Omega$, that contains the support of a Tchakaloff-like representation for L, i.e. $L(p) = \sum_{j=1}^{\nu} w_j\, p(t_j)\ \forall p \in S$, where $\nu \leq r$, $\{t_j\} \subset \mathcal{T}$ and $w_j > 0$ for every j.

Then, under the notations and assumptions above, Davis-Wilhelmsen theorem essentially asserts that

Theorem 2.1. *Let Ω, S and $L : S \to \mathbb{R}$ as above. Let $\{x_i\}_{i=1}^{\infty}$ be an everywhere dense subset of Ω. Then for sufficiently large k, the set $\{x_i\}_{i=1}^{k}$ is a Tchakaloff set for L on S.*

A consequence is that a subset

$$\mathcal{T}_k = \{x_1, \ldots, x_k\} \tag{13}$$

of a low-discrepancy sequence (like the Halton sequence) for k sufficiently large is a Tchakaloff set for the integral functional $I(p)$, $p \in \mathbb{P}_n^d$ (though a threshold for k is not given explicitly by the theorem and seems hard to determine analytically). This is in turn equivalent to the fact that the matching system with the continuous moments

$$V^t(\mathcal{T}_k)\, u = m_\Omega\,,\ \ V^t(\mathcal{T}_K) \in \mathbb{R}^{r\times k}\,,\ m_\Omega = \left\{I(p_j)\right\}_{1\leq j\leq r}\,, \tag{14}$$

and thus the NNLS problem $\min_{u\geq 0} \|V^t(\mathcal{T}_k)\, u - m_\Omega\|_2$, have a sparse solution if $k \geq r$ is large enough. Whenever the continuous moments are available or computable, the results above give a sound base to solve a sequence of "small" NNLS problems until the residual $\|V^t(\mathcal{T}_k)\, u - m_\Omega\|_2$ goes below a given tolerance. A similar strategy has been exploited in two recent papers, with spline-shaped and NURBS-shaped integration domains, where the polynomial moments can be computed by Gaussian quadrature along the boundary via the Gauss-Green theorem and the underdetermined systems to be solved by NNLS have small dimension, cf. [30, 32].

On the other hand, by Davis-Wilhelmsen theorem also the QMC functional $Q(p)$, $p \in \mathbb{P}_n^d$, has a Tchakaloff representation on a subset $\mathcal{T}_k = \{x_1, \ldots, x_k\}$ of a low-discrepancy sequence for k sufficiently large, provided that it is a strictly positive functional. This certainly holds whenever the low discrepancy set X is $\mathbb{P}_n^d$-determining, i.e. polynomials in $\mathbb{P}_n^d$ vanishing there vanish everywhere, a not really restrictive assumption for low-discrepancy sets with N sufficiently large as discussed above (cf. (7)).

Indeed we may expect that also the discrete moment-matching system

$$V^t(\mathcal{T}_k)\, u = m_X = V^t(X)\lambda = \{Q(p_j)\}\,,\ \lambda = \frac{vol(\Omega)}{N}(1, \ldots, 1)^t\,, \tag{15}$$

has a sparse nonnegative solution with number of nonzeros not exceeding r, for $k \geq r$ sufficiently large. That is, instead of solving directly the huge (3)-(4) problem, to compress the QMC cubature formula we may reduce to solve a sequence of "small" NNLS problems

$$\min_{u\geq 0} \|V^t(\mathcal{T}_{k_\ell})\, u - m_X\|_2\,,\ \ \ell = 0, 1, 2, \ldots\,, \tag{16}$$

until the residual $\|V^t(\mathcal{T}_{k_\ell})\, u - m_X\|_2$ goes below a given tolerance.

Some computational remarks are in order. First, notice that since X is a (low-discrepancy) sequence, we can take $\mathcal{T}_{k_\ell} \subset \mathcal{T}_N = X$ where k_ℓ is a subsequence with a given percentage of cardinality increase, like $k_{\ell+1} = (1+\theta)k_\ell$ with $k_0 \geq r$ (as a "rule of thumb", in our implementation we have chosen $k_0 = 8r$). Thus, once the Vandermonde-like matrix $V(X)$ has been constructed to compute the QMC moments m_X, the matrices $V(\mathcal{T}_{k_\ell})$ have not to be computed since they simply are $k_\ell \times N$ submatrices of $V(X)$.

Another possible bottleneck, that is computing the low-discrepancy set X when the size of N is huge (like N of the order of $10^5, 10^6$ and beyond), can be bypassed by precomputing and storing once and for all the points of a reference box, say $[0,1]^d$, and then loading and mapping the points by affine transformation into the smallest Cartesian box containing Ω. Of course a key aspect is then to have at hand a good "in-domain algorithm" for Ω, namely an efficient and robust implementation of the indicator function. While this can be straightforward when the domain is given by elementary set operations on standard components like discs and balls or other explicit sublevel sets, as well as polygons and polyhedra for which in-domain algorithms are available, the problem becomes much more difficult even with domains whose boundary is tracked by standard parametric curves. To this respect we may quote the recent paper [31], where an efficient implementation of the indicator function for 2D NURBS-shaped domains is provided.

In order to summarize the algorithm just described, we display below a Matlab function, named CQMC, that represents the core of the QMC compression procedure (for convenience we have numbered the instructions).

```
function [T,w,res]=CQMC(deg,X,vol,tol)

% computes a Compressed Quasi-Monte Carlo formula from a large
% low-discrepancy sequence on a low-dimensional compact set
% preserving the QMC polynomial moments up to a given degree,
% via Tchakaloff sets and NNLS moment-matching
```

```
% INPUT:
% deg: polynomial degree
% X: d-column array of a low-discrepancy sequence
% vol:  domain volume
% tol: moment-matching residual tolerance

% OUTPUT:
% T: compressed points (subset of X)
% w: corresponding positive weights
% res: moment-matching residual

% 1: preprocessing
% 1.1: cardinality of the low-discrepancy sequence
N=length(X(:,1));
% 1.2: Chebyshev-Vandermonde matrix of degree deg at X
V=dCHEBVAND(deg,X);
% 1.3: dimension of the polynomial space
r=length(V(1,:));
% 1.4: QMC moments
mom=V'*ones(N,1)*vol/N;

% 2: computing the compressed QMC formula
% 2.1: initializing the candidate Tchakaloff set cardinality
k=8*r;
% 2.2: initializing the residual
res=2*tol;
% 2.3: increase percentage of a candidate Tchakaloff set
theta=1;

% iterative search of a Tchakaloff set by NNLS moment-matching
while res>tol && k<=N
% 2.4: d-variate full-rank Chebyshev-Vandermonde matrix at X(1:k,:);
U=V(1:k,:);
% 2.5: polynomial basis discrete orthogonalization
[Q,R]=qr(U,0);
% 2.6: orthogonal moments
orthmom=(mom'/R)';
% 2.7: nonnegative weights by NNLS
w=lsqnonneg(Q',orthmom);
% 2.8: moment-matching residual
res=norm(U'*w-mom);
% 2.9: updating the candidate Tchakaloff set cardinality
k=floor((1+theta)*k);
end; % while

% compressed formula
% 2.10: indexes of the positive weights
ind=find(w>0);
% 2.11: compressed support points selection
T=X(ind,:);
% 2.12: corresponding positive weights
w=w(ind);
end % function
```

Some comments on the routine above are now in order. The first one is a preprocessing stage, where in **1.1**-**1.4** we begin by computing the QMC moments up to degree $n = \texttt{deg}$, and the Vandermonde-like matrix in the total-degree product Chebyshev basis with graded lexicographical ordering, scaled to the minimal Cartesian box containing the set X. To this purpose we resort to the Matlab function `dCHEBVAND` from the package [16].

In the second stage the QMC compression is performed via NNLS and the Lawson-Hanson active set algorithm [20]. Instead of compressing directly on the whole X, in **2.4**-**2.9** we implement (15)-(16), working with smaller matrices and seeking a small as possible Tchakaloff set. Here the matrix `U` corresponds to $V(\mathcal{T}_{k_\ell})$. We have here adopted the basic Matlab implementation of Lawson-Hanson algorithm given by the `lsqnonneg` function. Notice that a discrete orthogonalization of the polynomial basis is appropriate, to cope possible ill-conditioning that would affect Lawson-Hanson convergence (clearly, the moments have to be transformed correspondingly to the change of basis).

Finally, in **2.10**-**2.12** we select the nonvanishing weights (that are positive by construction) and the corresponding nodes which are a subset of X. In case the moment-matching tolerance is not reached, still in output we have a compressed formula with a moment-matching residual `res`.

3 Numerical examples

In this section we shall test the algorithm on some examples of area and volume integrals, obtaining substantial speed-ups by the present improved compression procedure given by Algorithm CQMC. In the general case when $vol(\Omega)$ is not known or easily computable (as in the examples below), we have adopted the QMC approximation

$$vol(\Omega) \approx vol(box)N/M\ , \tag{17}$$

where N/M is the fraction of M low-discrepancy points of a bounding box that are in Ω.

All the numerical tests of this section have been performed with a M1-chip PC with 16 GB of RAM, running Matlab R2021b. The Matlab codes and demos are freely available at https://www.math.unipd.it/~alvise/software.html.

3.1 Set operations with 2D NURBS-shaped domains

We begin with some 2D numerical examples, where we generate complex shapes by elementary set operations on curved domains whose boundary is tracked by NURBS. This is made possible by resorting to a quite recent effective implementation of the indicator function of 2D NURBS-shaped domains [31]. While on NURBS-shaped domains we have the capability of constructing positive algebraic cubature formulas [32], the situation changes drastically with union, intersection or set difference, where boundary tracking becomes a difficult problem. On the contrary, QMC cubature can be easily constructed and conveniently compressed.

For the purpose of illustration we consider complex shapes arising from union, intersection and symmetric difference of the two NURBS-shaped domains in Figure 1. All the numerical tests of this section have been performed with a M1-chip PC with 16 GB of RAM, running Matlab R2021b. The Matlab codes and demos are freely available at [18].

In Tables 1-3 we show the QMC compression parameters corresponding to $M = 10^6$ Halton points of minimal bounding boxes for the domains, at a sequence of polynomial exactness degrees. For notation clarity we have termed Q_c^{old} the NNLS compressed QMC formula on the whole X, whereas Q_c^{new} refers to the compressed QMC formula by Algorithm CQMC.

Observe that with the empirical inizialization $k_0 = 8r$, that has shown to be a good one for the degree ranges of all our 2D and 3D tests, Q_c^{new} performs at most 2 iterations and gives moment-matching residuals close to machine precision. Moreover, it turns out to be several times faster than Q_c^{old} (up to one order of magnitude), except at the highest degree, where however Q_c^{old} shows large residuals (labeled by a star), correspondingly to cases where the selected nodes are slightly less than the dimension of the exactness polynomial space.

In order to see the effect on polynomial exactness, in Fig. 2 we display as an example the relative errors

$$E^*(g_k) = \frac{|Q(g_k) - Q_c^*(g_k)|}{|Q(g_k)|}\ ,\ \ *= new, old, \tag{18}$$

corresponding to 100 trials of the polynomial

$$g_k = (a_k + b_k x + c_k y)^n \tag{19}$$

with uniform random coefficients $(a_k, b_k, c_k) \in [0,1]$, together with their logarithmic average $\sum_{k=1}^{100} \log(E^*(g_k))/100$, in the case of the union of two NURBS-shaped domains as in Fig. 1 top-left. Notice that for Q_c^{new} the latter slightly increases with the degree, remaining however not far from machine precision, as expected from the moment-matching residuals in Table 1. At the same time, for Q_c^{old} the loss of exactness due to much larger moment-matching residuals is manifest. Quite similar phenomena occur in the other cases, that we do not report for brevity.

In Table 4 we show the relative errors $E^*(f_i)$, $i = 1,2$, by the two compressed QMC with respect to the uncompressed one, on two test functions with different degree of regularity

$$f_1(P) = \exp(-|P - P_0|^2)\ ,\ \ f_2(P) = |P - P_0|^5\ , \tag{20}$$

where $P = (x, y)$ and $P_0 = (1, 0)$, in the case of the intersection of two NURBS-shaped domains as in Fig. 1 top-right. Again, the effect of lack of exactness of Q_c^{old} at the higher degrees is clearly visible on the Gaussian function (which is analytic).

3.2 Set operations with 3D elements

As it is known, the need of effective and simple to construct cubature formulas on curved polyhedral elements is still a challenging problem in the recent implementations of FEM and VEM, but is essential to keep the convergence order of the methods (that can be lost using linear polyhedral elements); cf., e.g., [1, 2, 6, 28] with the references therein. The difficulty of boundary tracking can be completely removed by QMC formulas, when the curved elements result from basic set operations of linear polyhedral elements with curved boundaries, as soon as the indicator function of the curved domain is computable. At the same time, no local element triangulation is needed.

As an example of potential application, we consider here a situation arising in computational mechanics, where curved elements can arise from the difference or the intersection of a standard tetrahedral mesh with a ball, in the presence of spherical holes within a homogeneous solid or spherical inclusions within a composite material, respectively (cf. [3] and the references therein for a similar 2D model). The moment-matching compression degrees are those most used in the FEM and VEM framework,

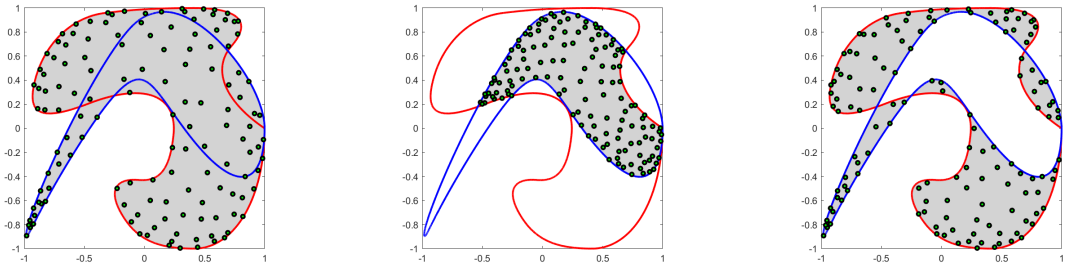

Figure 1: 231 compressed QMC nodes with exactness degree $n = 20$, on complex shapes arising from union (top-left), intersection (top-right) and symmetric difference (bottom) of two NURBS-shaped domains (extraction from a million Halton points of domain bounding boxes).

deg	5	10	15	20
$card(X) = 602015$				
card. Q_c^{old}	21	66	135	225
card. Q_c^{new}	21	66	136	231
compr. ratio	2.9e+04	9.1e+03	4.5e+03	2.7e+03
cpu Q_c^{old}	4.9e-01	2.2e+00	6.9e+00	1.9e+01
cpu Q_c^{new}	7.8e-02	2.5e-01	9.3e-01	1.8e+01
speed-up	6.3	8.9	7.4	1.0
mom. resid. Q_c^{old}	9.7e-16	1.7e-15	⋆ 8.4e-05	⋆ 1.9e-04
mom. resid. Q_c^{new}				
iter. 1	2.6e-16	1.2e-15	6.1e-02	2.2-04
iter. 2			1.4e-15	3.0e-15

Table 1: Compression parameters of QMC cubature with $N = 602015$ Halton points on the union of two NURBS-shaped domains as in Fig. 1 top-left.

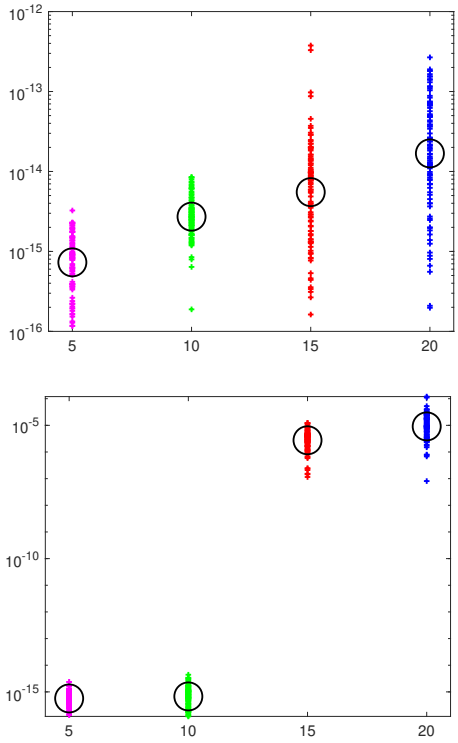

Figure 2: Relative QMC compression errors and their logarithmic average (circles) over 100 trials for Q_c^{new} (top) and Q_c^{old} (bottom) of random polynomials (19) on the union of Fig. 1-top left.

namely the even degrees 2, 4, 6 corresponding to the relevant scalar products involved by linear, quadratic or cubic piecewise polynomial functions.

In Fig. 3 we show 84 nodes for compressed QMC cubature produced by Algorithm CQMC for degree 6 on the intersection (red bullets) and difference (green bullets) of a tetrahedral element with a ball, starting from a million points of a bounding box.

deg	5	10	15	20
$card(X) = 255923$				
card. Q_c^{old}	21	66	133	226
card. Q_c^{new}	21	66	136	231
compr. ratio	1.2e+04	3.9e+03	1.9e+03	1.1e+03
cpu Q_c^{old}	2.4e-01	1.1e+00	3.1e+00	7.9e+00
cpu Q_c^{new}	4.0e-02	1.2e-01	2.8e-01	5.8e+00
speed-up	6.0	9.0	11.0	1.4
mom. resid. Q_c^{old}	8.1e-16	1.5e-15	⋆ 2.8e-05	⋆ 6.1e-05
mom. resid. Q_c^{new}				
iter. 1	5.8e-16	1.4e-15	1.5e+00	2.6e+00
iter. 2			2.4e-15	1.4e-01
iter. 3				7.0e-15

Table 2: Compression parameters of QMC cubature with $N = 255923$ Halton points on the intersection of two NURBS-shaped domains as in Fig. 1 top-right.

deg	5	10	15	20
$card(X) = 369831$				
card. Q_c^{old}	21	66	136	227
card. Q_c^{new}	21	66	136	231
compr. ratio	1.8e+04	5.6e+03	2.7+03	1.6e+03
cpu Q_c^{old}	2.9e-01	1.4e+00	4.3e+00	1.1e+01
cpu Q_c^{new}	4.9e-02	1.5e-01	3.2e-01	1.4e+01
speed-up	5.9	9.2	13.4	0.8
mom. resid. Q_c^{old}	1.2e-13	1.5e-15	2.2e-15	⋆ 1.0e-04
mom. resid. Q_c^{new}				
iter. 1	2.6e-16	1.2e-15	2.6e-01	4.9e+00
iter. 2			1.6e-15	1.4e-03
iter. 3				3.3e-15

Table 3: Compression parameters of QMC cubature with $N = 369831$ Halton points on the symmetric difference of two NURBS-shaped domains as in Fig. 1 bottom.

The compression parameters for degrees 2, 4, 6 are collected in Tables 4 and 5. We see that Q_c^{new} at these degrees is up to 8-9 times faster than Q_c^{old}, and that Q_c^{old} is not always able to produce extremely small residuals as Q_c^{new}. Similar results, that we do not report for brevity, are obtained also with more complicated polyhedral elements.

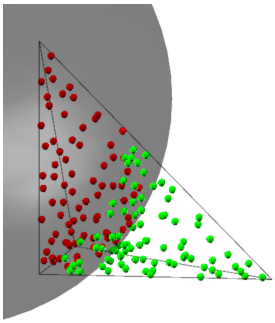

Figure 3: 84 compressed QMC nodes with exactness degree $n = 6$, on intersection (red bullets) and difference (green bullets) of a tetrahedral element with a ball (extraction from a million Halton points of domain bounding boxes).

Acknowledgements

This work was partially supported by the DOR funds and the biennial project BIRD 192932 of the University of Padova, and by the INdAM-GNCS 2022 Project "Methods and software for multivariate integral models", and has been accomplished within the RITA Research ITalian network on Approximation and the UMI Group TAA Approximation Theory and Applications.

References

[1] F. Aldakheel, B. Hudobivnik, E. Artioli, L. Beirão da Veiga and P. Wriggers, Curvilinear Virtual Elements for Contact Mechanics. *Comput. Methods Appl. Mech. Eng.*, 372, 2020.

[2] P. Antolin, X. Wei and A. Buffa, Robust Numerical Integration on Curved Polyhedra Based on Folded Decompositions. *Comput. Methods Appl. Mech. Eng.*, 395, 2022.

deg	5	10	15	20
$E^{old}(f_1)$	4.6e-05	1.9e-08	1.5e-06	4.6e-07
$E^{new}(f_1)$	2.7e-04	1.4e-08	3.0e-13	4.5e-16
$E^{old}(f_2)$	4.7e-04	4.5e-05	1.5e-05	2.5e-06
$E^{new}(f_2)$	2.3e-04	2.4e-05	1.1e-05	5.6e-06

Table 4: Relative QMC compression errors for the two test functions (20) on the intersection of Fig. 1 top-right.

deg	2	4	6
$card(X) = 216217$			
card. Q_c^{old}	10	35	84
card. Q_c^{new}	10	35	84
compr. ratio	2.2e+04	6.2e+03	2.6e+03
cpu Q_c^{old}	9.2e-02	3.4e-01	1.5e+00
cpu Q_c^{new}	4.1e-02	4.1e-02	1.8e-01
speed-up	2.2	8.3	8.2
mom. resid. Q_c^{old}	1.2e-15	1.9e-15	$\star$ 4.5e-07
mom. resid. Q_c^{new} iter. 1	1.7e-16	6.0e-16	1.2e-15

Table 5: Compression parameters of QMC cubature with $N = 216217$ Halton points on the intersection of a tetrahedral element with a ball as in Fig. 3.

[3] E. Artioli, A. Sommariva and M. Vianello, Algebraic cubature on polygonal elements with a circular edge. *Comput. Math. Appl.*, 79:2057–2066, 2020.

[4] B. Bauman, A. Sommariva and M. Vianello. Compressed cubature over polygons with applications to optical design. *J. Comput. Appl. Math.*, 370, 2020.

[5] B. Bauman and H. Xiao. Gaussian quadrature for optical design with noncircular pupils and fields, and broad wavelength range. *Proc. SPIE*, 7652(2): 1–12, 2010.

[6] L. Beirão da Veiga, A. Russo and G. Vacca, The Virtual Element Method with curved edges. *ESAIM Math. Model. Numer. Anal.*, 53, 2019.

[7] L. Bittante, S. De Marchi and G. Elefante. A new quasi-Monte Carlo technique based on nonnegative least-squares and approximate Fekete points. *Numer. Math. Theory Methods Appl.*, 9: 640–663, 2016.

[8] L. Brandolini, L. Colzani, G. Gigante and G. Travaglini. On the Koksma-Hlawka inequality. *J. Complexity*, 29: 158–172, 2013.

[9] R.E. Caflisch, Monte Carlo and quasi-Monte Carlo methods. *Acta Numerica*, 7: 1–49, 1998.

[10] J.P. Calvi and N. Levenberg. Uniform approximation by discrete least squares polynomials. *J. Approx. Theory*, 152: 92–100, 2008.

[11] C. Caratheodory. Uber den Variabilittsbereich der Fourierschen Konstanten von positiven harmonischen Funktionen. *Rend. Circ. Mat. Palermo*, 32:193–217, 1911.

[12] R. Cavoretto, A. De Rossi. Software for Approximation 2022 (SA2022). *Dolomites Res. Notes Approx.*, Special Issue SA2022, 15:i–ii, 2022.

[13] P.J. Davis, A construction of nonnegative approximate quadratures. *Math. Comp.*, 21:578–582, 1967.

[14] F. Dell'Accio, F. Di Tommaso, N. Siar and M. Vianello, DISC: an adaptive numerical Differentiator by local polynomial Interpolation on multivariate SCattered data. *Dolomites Res. Notes Approx.*, Special Issue SA2022, 15:81–91, 2022.

[15] S. De Marchi and G. Elefante. Quasi-Monte Carlo integration on manifolds with mapped low-discrepancy points and greedy minimal Riesz s-energy points. *Appl. Numer. Math.*, 127: 110–124, 2018.

[16] M. Dessole, F. Marcuzzi, A. Sommariva and M. Vianello. dCATCH: numerical package for d-variate discrete measure compression, near-optimal design and polynomial fitting, v1.1 (2020). Available online at: https://www.math.unipd.it/~marcov/dCATCH.html.

[17] J. Dick and F. Pillichshammer, Digital Nets and Sequences. Discrepancy Theory and Quasi-Monte Carlo Integration. Cambridge University Press, Cambridge, 2010.

[18] G. Elefante, A. Sommariva and M. Vianello. CQMC: a software package for low-dimensional Compressed Quasi-MonteCarlo cubature, v0.1 (June 2022). Available online at https://www.math.unipd.it/~alvise/software.html.

[19] S. Hayakawa. Monte Carlo cubature construction. *Jpn. J. Ind. Appl. Math.*, 38:561–577, 2021.

[20] C.L. Lawson and R.J. Hanson. Solving least squares problems. *SIAM Classics in Applied Mathematics 15*, Philadelphia, 1995.

[21] C. Litterer and T. Lyons. High order recombination and an application to cubature on Wiener space. *Ann. Appl. Probab.*, 22:1301–1327, 2012.

[22] F. Pausinger and A.M. Svane. A Koksma-Hlawka inequality for general discrepancy systems. *J. Complexity*, 31: 773–797, 2015.

[23] M. Petitjean. Spheres Unions and Intersections and Some of their Applications in Molecular Modeling. *A. Mucherino & al., Eds., Distance Geometry: Theory, Methods, and Applications., Springer New York*, pp.61-83, 2013.

[24] W. Plésniak, Multivariate Jackson Inequality. *J. Comput. Appl. Math.*, 233:815–820, 2009.

[25] F. Piazzon, A. Sommariva and M. Vianello. Caratheodory-Tchakaloff Subsampling. *Dolomites Res. Notes Approx. DRNA*, 13:5–14, 2017.

[26] E.K. Ryu and S.P. Boyd. Extensions of Gauss quadrature via linear programming. *Found. Comput. Math.*, 15:953–971, 2015.

deg	2	4	6
$card(X) = 58561$			
card. Q_c^{old}	10	35	84
card. Q_c^{new}	10	35	84
compr. ratio	5.9e+03	1.7e+03	7.0e+02
cpu Q_c^{old}	1.1e-01	1.4e-01	4.5e-01
cpu Q_c^{new}	3.3e-02	2.1e-02	5.5e-02
speed-up	3.4	6.9	8.8
mom. resid. Q_c^{old}	4.1e-16	9.2e-16	2.1e-15
mom. resid. Q_c^{new}			
iter. 1	5.0e-16	6.1e-16	1.2e-15

Table 6: Compression parameters of QMC cubature with $N = 58561$ Halton points on the difference of a tetrahedral element with a ball as in Fig. 3.

[27] R. Sevilla and S. Fernández-Méndez, Numerical integration over 2D NURBS-shaped domains with applications to NURBS-enhanced FEM. *Finite Elem. Anal. Des.*, 47: 1209–1220, 2011.

[28] R. Sevilla, S. Fernández-Méndez and A. Huerta, 3D NURBS-enhanced finite element method (NEFEM). *Int. J. Numer. Meth. Eng.*, 88(2): 103–125, 2021.

[29] A. Sommariva, M. Vianello. Compression of multivariate discrete measures and applications. *Numer. Funct. Anal. Optim.*, 36:1198–1223, 2015.

[30] A. Sommariva, M. Vianello. Computing Tchakaloff-like cubature rules on spline curvilinear polygons. *Dolomites Res. Notes Approx. DRNA*, 14: 1–11, 2021.

[31] A. Sommariva, M. Vianello. inRS: implementing the indicator function of NURBS-shaped planar domains. *Appl. Math. Lett.*, 130, (2022).

[32] A. Sommariva, M. Vianello. Low-cardinality Positive Interior cubature on NURBS-shaped domains. *Preprint*, 2022. Available online at: https://www.math.unipd.it/~marcov/pdf/nurbscatch.pdf.

[33] V. Tchakaloff. Formules de cubatures mécaniques à coefficients non négatifs, (French). *Bull. Sci. Math.*, 81:123–134, 1957.

[34] M. Tchernychova. "Caratheodory" cubature measures. Ph.D. dissertation in Mathematics (supervisor: T. Lyons), University of Oxford, 2015.

[35] D.R. Wilhelmsen, A Nearest Point Algorithm for Convex Polyhedral Cones and Applications to Positive Linear approximation. *Math. Comp.*, 30:48–57, 1976.

[36] Q. Zhang. On donating regions: Lagrangian flux through a fixed curve. *SIAM Rev.*, 55:443–461, 2013.